Available online at www.sciencedirect.com
SCIENCE DIRECT®
ELSEVIER
Journal of Solid State Chemistry 179 (2006) 1363–1368
JOURNAL OF SOLID STATE CHEMISTRY
www.elsevier.com/locate/jssc

Single crystal structure and Raman spectrum of $Ba_3Na_2(CN_2)_4$

Yongkwan Dong, Francis J. DiSalvo*

Department of Chemistry and Chemical Biology, Baker Laboratory, Cornell University, Ithaca, NY 14853-1301, USA

Received 8 December 2005; received in revised form 26 January 2006; accepted 27 January 2006
Available online 28 February 2006

Abstract

The synthesis, single crystal structure determination, and Raman spectrum are reported for colorless transparent tribarium disodium tetracyanamide, $Ba_3Na_2(CN_2)_4$. The title compound crystallizes in the space group $C_{2h}{}^5$-$P2_1/c$ (#14, $a = 6.2872(5)$ Å, $b = 10.0002(8)$ Å, $c = 17.7303(16)$ Å, $\beta = 110.454(4)°$, $V = 1044.48(15)$ Å^3, $Z = 4$, $R/wR = 0.0266/0.0543$). Each sodium atom is surrounded by six nitrogen atoms in octahedral geometry. Sodium centered nitrogen octahedra are linked through face-sharing along the [100] direction to form one-dimensional (1D) chains. These chains are connected to each other through the carbon atoms of cyanamide and make a three-dimensional (3D) network with 1D channels along the [100] direction. Barium atoms and additional cyanamide anions reside in the channels. Each barium atom is irregularly coordinated with nitrogen and carbon from the cyanamide anions. The Raman spectrum shows symmetric vibrations of $[N{=}C{=}N]^{2-}$ corresponding to ν_{sym} (1241.5 cm^{-1}) and 2δ (1356.4 cm^{-1}).

Keywords: Barium; Sodium; Cyanamide; Crystal structure; Raman spectrum

1. Introduction

Subnitrides containing alkali and alkaline-earth metals such as $NaBa_3N$ [1], Na_5Ba_3N [2], and $Na_{16}Ba_6N$ [3] have attracted attention because of their unusual physical and chemical properties. The structure of these compounds can be described as a metallic region of Na separated by isolated $[Ba_6N]$ octahedra or infinite $^1_\infty[Ba_3N]$ chains with Ba–N ionic bonding. From theoretical studies [4], these compounds are expected to be metallic due to Na–Na and Na–Ba metallic bonding.

In ternary or quaternary subnitrides containing gallium or indium, these metals form isolated Zintl anions instead of bonding to N atoms. The variety of M ($M = $ Ga, In) arrangements extend to isolated M atoms [5], isolated cluster units such as $[In_4]^{8-}$, $[Ga_5]^{7-}$, $[In_5]^{5-}$, and $[In_8]^{12-}$ [6–10], 1D infinite zigzag chains or cluster chains [11–15], and a 3D network of corner-sharing tetracapped tetrahedra [16]. NaSnN [17], which has been synthesized from a NaSn intermetallic phase under flowing NH_3 gas (ammonolysis), shows a novel layered Zintl anion $[SnN]^-$ with Sn–N bonding. Sn also can act like Ga or In in Zintl-like phases. For this reason, we were interested to extend subnitride chemistry to Sn containing nitrides. In attempts to synthesize a quaternary sodium–barium–tin-nitride, we obtained the title compound as a by-product.

Cyanamide compounds [18–20] are sometimes obtained unintentionally due to carbon impurities in reaction tubes (Nb or Ni container) or in one or more of the reactants. However, recently cyanamide and its salts have fascinated attention due to their solid-state coordination chemistry as well as molecular chemistry. Up to now, while binary cyanamides, $M_x(CN_2)_y$ (M is usually alkali, alkaline earth, or main-group elements), have been synthesized and structurally characterized, known ternary cyanamides are rare. Here we report the single-crystal structure and Raman spectrum of the ternary cyanamide, $Ba_3Na_2(CN_2)_4$.

2. Experimental section

2.1. Synthesis

All manipulations were performed in an argon-filled glovebox. In an attempt to prepare new multinary nitrides using Sn as a reactant and as a flux, the compound

---

*Corresponding author. Fax: +1 607 255 4137.
E-mail address: fjd3@cornell.edu (F.J. DiSalvo).

0022-4596/$ - see front matter © 2006 Elsevier Inc. All rights reserved.
doi:10.1016/j.jssc.2006.01.048

$Ba_3Na_2(CN_2)_4$ was obtained by the reaction of $Ba(N_3)_2$ and NaN_3. The starting materials of 0.1107 g of $Ba(N_3)_2$ [21], 0.1187 g of Sn (JohnsonMatthey, 99.9%), and 0.0325 g of NaN_3 (Aldrich, 99%) were placed into a Nb tube which was made by welding one end of a Nb tube in an argon atmosphere, using a Centorr Associates arc furnace. The atomic ratio of Ba/Na/Sn was 1:1:2. After the remaining end of the Nb tube was welded closed, the reaction tube was put into silica container and sealed under vacuum to prevent oxidation of the reaction tube during heating. The reaction tube was heated gradually to 800 °C over 24 h and held at this temperature for 72 h. The tube was cooled to room temperature at 3 °C/h. Metallic block crystals and only one colorless transparent needle crystal were found in the batch. The former crystals were the major phase and proved to be Ba_3Sn_5 [22] by means of single crystal diffraction. The title compound is somewhat air sensitive but is stable in polybutene oil over several days.

Unfortunately, single-phase material could not be obtained by changing the starting materials such as Ba_2N, NaN_3, and C or $BaCN_2$ and Na_2CN_2 or the reaction temperature. It is likely that the carbon in the cyanamide anions comes adventitiously from the niobium tube or one or more starting reactants as mentioned by Reckeweg and DiSalvo [18].

2.2. *Crystallographic studies*

Samples of the reaction mixture were removed from the glovebox in polybutene oil for single-crystal selection. The colorless transparent needle crystal was manually selected from the reaction mixture, mounted in a drop of polybutene oil sustained in a plastic loop, and placed onto the goniometer. A cold stream of nitrogen froze the polybutene oil, thus keeping the crystal stationary and protected from oxygen and moisture in the air.

Preliminary examination and data collection were performed on a Bruker X8 Apex II diffractometer equipped with 4 K CCD detector and graphite-monochromatized Mo*K*α radiation ($\lambda = 0.7107$ Å). The initial monoclinic cell constants ($a = 6.2872(5)$ Å, $b = 10.0002(8)$ Å, $c = 16.6127(15)$ Å, $\beta = 90.314(4)^\circ$, and $V = 1044.5(2)$ Å^3) and orientation matrix were obtained by using APEX2 [23]. The program SAINT was used to integrate the data [24]. An empirical absorption correction was applied using SADABS [25]. The initial input file for solving the crystal structure was prepared by XPREP [26]. XPREP suggested only one possible space group, $P2_1/n$, for the crystal structure. The systematic absences ($h0l$: $h + l = 2n + 1$ and $0k0 : k = 2n + 1$) are consistent with the monoclinic space group, $C_{2h}{}^5$-$P2_1/n$. The distribution of normalized structure factor (*E*-values, $\langle E^2 - 1\rangle = 0.959$) indicates that the structure should be centrosymmetric. However, after solving the crystal structure in $P2_1/n$, the ADDSYM algorithm in the PLATON program package suggested the standard setting for this space group $P2_1/c$ with the transformation matrix $(100,\ 0\bar{1}0,\ \bar{1}0\bar{1})$ for this structure [27,28]. The satisfactory refinement confirmed the choice of this space group. The initial positions for all atoms were obtained by using direct methods in SHELXS97 [29] and the structure was refined by full-matrix least-squares techniques with the use of the SHELXL97 [29] in the WinGX program package [30]. The atomic parameters were standardized by using STRUCTURE TIDY [31]. The final cycle of refinement performed on F_o^2 with 5015 unique reflections afforded residuals w$R_2 = 0.0543$ and a conventional R index based on 3805 reflections having $F_o^2 > 2\sigma(F_o^2)$ of 0.0266. The highest peak and deepest hole are located 1.13 and 0.60 Å from atoms Ba2 and Ba3, respectively, and are due to data truncation errors ($2\theta_{max} = 72.5^\circ$). Additional crystallographic details are described in Table 1. Atomic coordinates as well as isotropic displacement coefficients are listed in Table 2. Final anisotropic displacement parameters and selected bond distances and angles are given in Tables 3 and 4, respectively. Further details of the crystal structure investigation can be obtained from the Fachinformationszentrum Karlsruhe, 76344 Eggenstein-Leopoldshafen, Germany (fax: +49 7247 808 666; E-mail: crysdata@fiz-karlsruhe.de) on quoting the depository number CSD-416033.

2.3. *Raman spectroscopy and microprobe analysis*

After the X-ray diffraction measurements, the crystal was retrieved for elemental analysis and a vibrational study. A microprobe analysis of the colorless transparent needle crystal was made with an EDAX (Thermonoran) equipped scanning electron microscope (Jeol JXA-8900R). EDAX analysis of this crystal indicated the presence of Ba, and Na and no other elements were detected with $Z \geqslant 10$. To prevent decomposition of the sample, the title

Table 1
Details of X-ray data collection and refinement for $Ba_3Na_2(CN_2)_4$

Formula weight (amu)	618.12
Space group	$C_{2h}{}^5$–$P2_1/c$ (#14)
a (Å)	6.2872(5)
b (Å)	10.0002(8)
c (Å)	17.7303(16)
β (deg)	110.454(4)
V (Å^3)	1044.48(15)
Z	4
T (K)	167.0(1)
Radiation	Graphite monochromated Mo*K*α ($\lambda(K\alpha) = 0.7107$ Å)
Linear absorption coefficient (mm^{-1})	11.253
Density (calc. g/cm^3)	3.931
Crystal size (mm^3)	0.28 × 0.04 × 0.04
θ limits (deg)	$2.38^\circ \leqslant \theta \leqslant 36.23^\circ$
Data collected	$-10 \leqslant h \leqslant 10$, $-16 \leqslant k \leqslant 16$, $-29 \leqslant l \leqslant 27$
No. of unique data with F_o^2	5015 ($R_{int} = 0.0462$)
No. of parameters	157
No. of unique data with $F_o^2 > 2\sigma(F_o^2)$	3805
wR_2 ($F_o^2 > 0$)	0.0543
R_1 (on F_o for $F_o^2 > 2\sigma(F_o^2)$)	0.0266
Goodness-of-fit on F^2	0.986
Min. and max. residual e-density (e/Å^3)	−2.619 and 1.884

Table 2
Atomic coordinates and equivalent isotropic displacement parameters (Å^2) for $Ba_3Na_2(CN_2)_4$

Atoms	Wyckoff notation	x	Y	z	U_{eq}[a]
Ba(1)	4e	0.1059(1)	0.3738(1)	0.3574(1)	0.010(1)
Ba(2)	4e	0.4136(1)	0.1809(1)	0.1545(1)	0.009(1)
Ba(3)	4e	0.7658(1)	0.3108(1)	0.0066(1)	0.009(1)
Na(1)	4e	0.1079(2)	0.5235(1)	0.1700(1)	0.011(1)
Na(2)	4e	0.3895(2)	0.0215(1)	0.3310(1)	0.011(1)
C(1)	4e	0.0447(4)	0.7231(3)	0.2993(2)	0.009(1)
C(2)	4e	0.2568(4)	0.3953(2)	0.0027(2)	0.009(1)
C(3)	4e	0.5613(4)	0.3275(2)	0.3096(2)	0.008(1)
C(4)	2b	0.5	0	0	0.009(1)
C(5)	2a	0	0	0	0.009(1)
N(1)	4e	0.0654(4)	0.1211(2)	0.2282(2)	0.012(1)
N(2)	4e	0.1510(4)	0.8268(2)	0.3239(2)	0.011(1)
N(3)	4e	0.2425(4)	0.4199(2)	0.0689(1)	0.011(1)
N(4)	4e	0.2704(4)	0.1216(2)	0.4355(2)	0.013(1)
N(5)	4e	0.4465(4)	0.4247(2)	0.2767(1)	0.013(1)
N(6)	4e	0.6707(4)	0.2252(2)	0.3382(2)	0.014(1)
N(7)	4e	0.6045(4)	0.0792(2)	0.0531(1)	0.013(1)
N(8)	4e	0.0640(4)	0.1168(2)	0.0126(2)	0.014(1)

[a] $\underline{U}_{eq}$ is defined as one-third of the trace of the orthogonalized U_{ij} tensor.

Table 3
Anisotropic displacement parameters (Å^2) for $Ba_3Na_2(CN_2)_4$

Atoms	U_{11}	U_{22}	U_{33}	U_{23}	U_{13}	U_{12}
Ba(1)	0.011(1)	0.011(1)	0.008(1)	0.000(1)	0.003(1)	−0.001(1)
Ba(2)	0.010(1)	0.009(1)	0.008(1)	0.000(1)	0.003(1)	0.000(1)
Ba(3)	0.009(1)	0.009(1)	0.007(1)	0.000(1)	0.002(1)	0.000(1)
Na(1)	0.013(1)	0.012(1)	0.009(1)	0.000(1)	0.003(1)	0.000(1)
Na(2)	0.010(1)	0.012(1)	0.009(1)	0.000(1)	0.002(1)	0.000(1)
C(1)	0.008(1)	0.013(1)	0.005(1)	0.001(1)	0.002(1)	0.003(1)
C2)	0.006(1)	0.006(1)	0.013(1)	0.000(1)	0.001(1)	−0.001(1)
C(3)	0.010(1)	0.010(1)	0.006(1)	−0.003(1)	0.004(1)	−0.003(1)
C(4)	0.011(2)	0.008(2)	0.011(2)	0.003(1)	0.006(1)	0.002(1)
C(5)	0.010(2)	0.012(2)	0.004(2)	0.002(1)	0.002(1)	0.004(1)
N(1)	0.012(1)	0.013(1)	0.012(1)	0.000(1)	0.004(1)	0.001(1)
N(2)	0.014(1)	0.010(1)	0.012(1)	0.000(1)	0.006(1)	0.001(1)
N(3)	0.013(1)	0.011(1)	0.009(1)	0.000(1)	0.002(1)	0.000(1)
N(4)	0.012(1)	0.015(1)	0.011(1)	−0.002(1)	0.004(1)	0.001(1)
N(5)	0.015(1)	0.011(1)	0.013(1)	0.000(1)	0.004(1)	0.001(1)
N(6)	0.014(1)	0.015(1)	0.011(1)	0.002(1)	0.004(1)	0.002(1)
N(7)	0.013(1)	0.013(1)	0.012(1)	−0.001(1)	0.005(1)	−0.001(1)
N(8)	0.012(1)	0.013(1)	0.016(1)	−0.002(1)	0.004(1)	−0.001(1)

Note: The anisotropic displacement factor exponent takes the form: $-2\pi^2[h^2a^{*2}U_{11} + k^2b^{*2}U_{22} + l^2c^{*2}U_{33} + 2klb^*c^*U_{23} + 2hla^*c^*U_{13} + 2hka^*b^*U_{12}]$.

Table 4
Selected bond lengths (Å) and angles (°) for $Ba_3Na_2(CN_2)_4$

Ba(1)–N(1)#3	2.905(2)	Ba(2)–N(1)	2.975(2)
Ba(1)–N(2)#4	3.088(2)	Ba(2)–N(2)#6	3.007(2)
Ba(1)–N(4)	2.889(2)	Ba(2)–N(3)	2.834(2)
Ba(1)–N(5)	3.005(2)	Ba(2)–N(5)	3.220(2)
Ba(1)–N(6)#5	3.026(2)	Ba(2)–N(5)#6	2.842(2)
Ba(1)–N(7)#1	2.834(2)	Ba(2)–N(6)	3.120(2)
Ba(1)–N(8)#2	2.857(3)	Ba(2)–N(7)	2.686(2)
Ba(1)–C(1)#4	3.008(3)	Ba(2)–N(8)	2.776(2)
Ba(1)–C(3)	3.290(3)	Ba(2)–C(1)#6	3.241(2)
Ba(1)–C(3)#5	3.260(3)	Ba(2)–C(1)#4	3.286(3)
Ba(1)–C(4)#1	3.1223(3)	Ba(2)–C(2)	3.310(3)
Ba(1)–C(5)#3	3.0996(3)	Ba(2)–C(3)	2.964(3)
Ba(3)–N(2)#6	2.868(2)	Na(1)–N(1)#3	2.603(3)
Ba(3)–N(3)#7	3.013(2)	Na(1)–N(2)#4	2.579(2)
Ba(3)–N(3)#9	3.000(2)	Na(1)–N(3)	2.462(3)
Ba(3)–N(4)#1	3.307(2)	Na(1)–N(4)#3	2.648(3)
Ba(3)–N(4)#8	3.001(2)	Na(1)–N(5)	2.505(3)
Ba(3)–N(6)#8	2.857(2)	Na(1)–N(6)#1	2.483(3)
Ba(3)–N(7)	2.767(2)		
Ba(3)–N(8)#7	2.674(2)	Na(2)–N(1)	2.423(3)
Ba(3)–C(1)#6	3.341(3)	Na(2)–N(2)#10	2.434(2)
Ba(3)–C(2)	3.287(2)	Na(2)–N(3)#6	2.582(3)
Ba(3)–C(2)#7	3.225(2)	Na(2)–N(4)	2.442(3)
Ba(3)–C(2)#9	2.945(2)	Na(2)–N(5)#6	2.650(3)
		Na(2)–Na(6)	2.671(3)
Na(1)–Na(2)#1	3.1660(14)	Na(1)–Na(2)#3	3.1214(14)
C(1)–N(1)#3	1.233(3)	C(2)–N(3)	1.232(3)
C(1)–N(2)	1.229(3)	C(2)–N(4)#8	1.237(3)
C(3)–N(5)	1.229(3)	C(4)–N(7) × 2	1.230(2)
C(3)–N(6)	1.238(3)	C(5)–N(8) × 2	1.230(2)
N(1)#3–Na(1)–N(2)#4	80.44(8)	N(1)–Na(2)–N(2)#10	87.08(8)
N(1)#3–Na(1)–N(3)	175.17(9)	N(1)–Na(2)–N(3)#6	174.24(9)
N(1)#3–Na(1)–N(4)#3	81.96(8)	N(1)–Na(2)–N(4)	90.11(9)
N(1)#3–Na(1)–N(5)	94.34(8)	N(1)–Na(2)–N(5)#6	92.55(9)
N(1)#3–Na(1)–N(6)#1	96.59(8)	N(1)–Na(2)–N(6)	95.21(8)
N(2)#4–Na(1)–N(3)	95.28(8)	N(2)#10–Na(2)–N(3)#6	96.24(8)
N(2)#4–Na(1)–N(4)#3	83.55(8)	N(2)#10–Na(2)–N(4)	91.16(9)
N(2)#4–Na(1)–N(5)	92.87(8)	N(2)#10–Na(2)–N(5)#6	93.34(8)
N(2)#4–Na(1)–N(6)#1	175.22(9)	N(2)#10–Na(2)–N(6)	176.55(9)
N(3)–Na(1)–N(4)#3	95.40(8)	N(3)#6–Na(2)–N(4)	94.52(9)
N(3)–Na(1)–N(5)	88.08(8)	N(3)#6–Na(2)–N(5)#6	82.58(8)
N(3)–Na(1)–N(6)#1	87.54(9)	N(3)#6–Na(2)–N(6)	81.27(8)
N(4)#3–Na(1)–N(5)	175.21(9)	N(4)–Na(2)–N(5)#6	174.88(9)
N(4)#3–Na(1)–N(6)#1	92.36(8)	N(4)–Na(2)–N(6)	91.42(8)
N(5)–Na(1)–N(6)#1	91.08(8)	N(5)#6–Na(2)–N(6)	83.99(8)
N(1)#3–C(1)–N(2)	177.6(3)	N(7)–C(4)–N(7)#11	180.0(3)
N(3)–C(2)–N(4)#8	176.3(3)	N(8)–C(5)–N(8)#12	180.00(6)
N(5)–C(3)–N(6)	175.9(3)		

Symmetry transformations used to generate equivalent atoms: #1 $-x+1$, $y+1/2$, $-z+1/2$, #2 x, $-y+1/2$, $z+1/2$, #3 $-x$, $y+1/2$, $-z+1/2$, #4 $-x$, $y-1/2$, $-z+1/2$, #5 $x-1$, y, z, #6 $-x+1$, $y-1/2$, $-z+1/2$, #7 $x+1$, y, z, #8 x, $-y+1/2$, $z-1/2$, #9 $-x+1$, $-y+1$, $-z$, #10 x, $y-1$, z, #11 $-x+1$, $-y$, $-z$, #12 $-x$, $-y$, $-z$, #13 x, $y+1$, z.

compound was transferred from an Ar-filled glove box to the microprobe using a specially designed portable antechamber [32].

The Raman investigations were carried out with a microscope laser Raman spectrometer (Dilor XY 800 Raman system using the 514.532 nm excitation line of an argon-ion laser in a back scattering mode, 100 × magnification, 2 × 300 s accumulation time). The single crystal remained in the polybutene oil. The resulting Raman spectrum for $Ba_3Na_2(CN_2)_4$ is shown in Fig. 4.

3. Results and discussion

The title compound, $Ba_3Na_2(CN_2)_4$, crystallizes in the monoclinic space group $P2_1/c$, with three independent positions for Ba, two for Na, five for C, and eight for N atoms. The perspective view of the $Ba_3Na_2(CN_2)_4$ crystal structure along the [100] direction is illustrated in Fig. 1. Each sodium atom is surrounded by six nitrogen atoms in nearly octahedral geometry (Fig. 2). Sodium centered nitrogen octahedra are linked through face-sharing along the [100] direction and make 1D chains. These chains are connected to each other to form a 3D network, ${}^{3}_{\infty}[Na_2(CN_2)_3]^{4-}$, through the carbon atoms of cyanamide resulting in 1D channels along the [100] direction. Barium atoms and additional cyanamide units reside in the channels. Each barium atom is irregularly coordinated with nitrogen and carbon atoms of the cyanamide anions. Ba1 is coordinated to seven nitrogen atoms and five carbon atoms. Ba2 and Ba3 are coordinated to eight nitrogen atoms and four carbon atoms. The reported average bond distances between Ba and N or C are 2.917 Å for Ba–N in $Ba(N_3)_2$ [21] and 3.057 Å for Ba–C in monoclinic BaC_2 [33]. Thus, if the bond distances arbitrarily cut off at 3.1 Å, Ba1 is bonded to seven nitrogen and two carbon atoms in a bicapped pentagonal bipyramid, Ba2 is linked by six nitrogen and one carbon atoms in highly distorted pentagonal bipyramid, and Ba3 is surrounded by seven nitrogen atoms and one carbon atom in highly distorted monocapped pentagonal bipyramid (Fig. 3).

Selected bond distances and angles are listed in Table 4. The Na···Na distances alternate between 3.1660(14) and 3.1214(14) Å along the chain direction. The sum of these two values corresponds to the crystallographic *a*-axis length. These distances are somewhat shorter than those in Na_2CN_2 (3.184(1)–3.245(1) Å) [34] due to different geometries. The Na–N distances range from 2.462(3) to 2.648(3) Å for Na1 and from 2.423(3) to 2.671(3) Å for Na2. These values are similar to those in Na_2CN_2 (2.412(1) to 2.618(1) Å) and comparable to the sum of the ionic radii of each element (2.48 Å; $Na^+ = 1.02$ Å, $N^{3-} = 1.46$ Å) [35]. However, the Na–N bond distances of the title

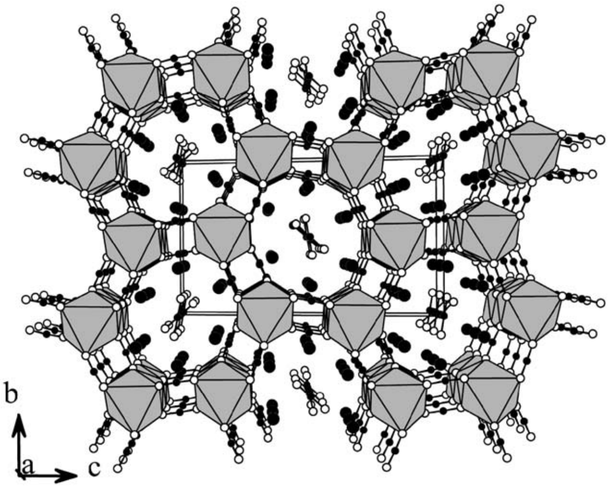

Fig. 1. Perspective view of $Ba_3Na_2(NCN)_4$ along the [100] direction. Large black circles are Ba atoms; small black circles are C atoms; small open circles are N atoms; Na atoms are inside the polyhedra. The bondings between Ba and C or N have been omitted for clarity.

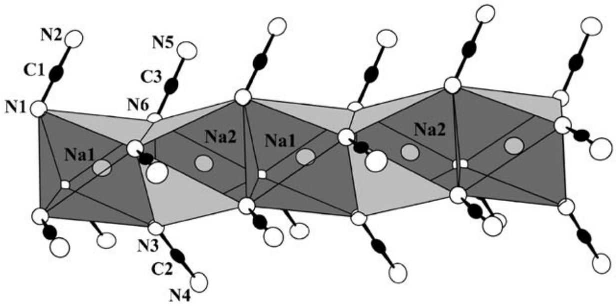

Fig. 2. Individual 1D chain of sodium centered nitrogen face-sharing octahedra parallel to the [100] direction. Displacement ellipsoids are drawn at the 90% probability level.

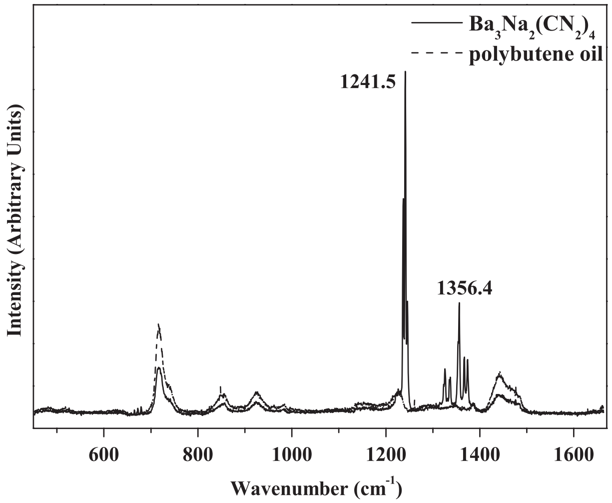

Fig. 4. Raman spectrum of $Ba_3Na_2(NCN)_4$. Solid line is $Ba_3Na_2(NCN)_4$ and dashed line is polybutene oil.

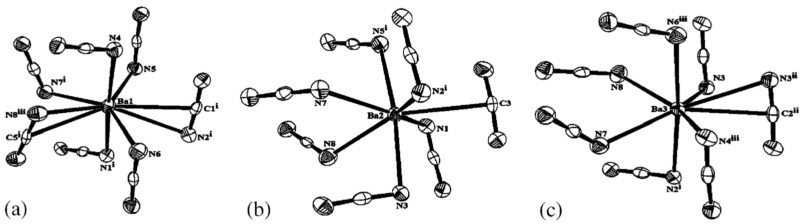

Fig. 3. ORTEP drawing of each Ba atom coordination environments: (a) Ba1, (b) Ba2, and (c) Ba3. Displacement ellipsoids are drawn at the 90% probability level. [Symmetry codes: (i) $-x$, $0.5+y$, $0.5-z$, (ii) $-x$, $-y$, $-z$, and (iii) x, $0.5-y$, $0.5+z$.]

Table 5
Comparison of vibrational frequencies between $Ba_3Na_2(CN_2)_4$ and other related cyanamides

	$Ba_3Na_2(CN_2)_4$	$Ba_2Na(CN_2)(CN)_3$ [38]	$BaCN_2$ [37]	Na_2CN_2 [34]
d(C–N) (Å)	1.228(3)–1.230(3)	1.223(7)	119.2(11)	1.236(1)
∠N–C–N (deg)	176.0(3)–180.0(2)	180.0(1)	177.2(18)	179.9
$\nu_{\text{sym.}}$ (cm^{-1})	1237/1242/1246	1259	1238	1242
$\nu_{\text{asym.}}$ (cm^{-1})	Not measured	1971	1947	2008
δ (cm^{-1})	665/672/679	670	662/673	662/672
2δ (cm^{-1})	1326/1337/1356/1367/1374	1363	~1300	

compound are slightly longer than those in Na_3N (2.366 Å) [36] because the environment of the N is quite different (NaN_6 octahedron ($Ba_3Na_2(CN_2)_4$) vs. Na_6N octahedron (Na_3N)).

There are five crystallographically independent cyanamide anions in the title compound. All C–N double bond distances range from 1.229(3) to 1.238(3) Å, in good agreement with other cyanamides [18–20,33,37,38]. In two cyanamide anions, the central C atoms (C4 and C5) occupy a center of symmetry and the four N atoms are generated by only two crystallographic sites (N7 and N8) resulting in $D_{\infty h}$ point group with N–C–N bond angle of 180.0°. The other observed N–C–N bond angles of 175.9(3)°, 176.3(3)°, and 177.6(3)° indicate a reduction of symmetry from $D_{\infty h}$ to C_{2v}.

In the first stages of the structure refinement, we refined the crystal structure assuming the anion was an azide. In binary A or Ae azide compounds (A = alkali metals; Ae = alkaline earth metals), bond distances between N atoms are normally around 1.17 Å. However, bond distances between C atoms and N atoms in cyanamide are about 0.06 Å larger and are closer to the observed distances in the title compound. While the charge balance with an azide ($[Ba^{2+}]_3[Na^+]_2[N_3^-]_4$), is not exact and would result in metallic behavior, the cyanamide model results in exact charge balance ($[Ba^{2+}]_3[Na^+]_2[N=C=N^{2-}]_4$) and is consistent with the transparent colorless appearance of the crystal. To confirm the existence of cyanamide anions, we performed Raman spectroscopy. The symmetric stretch modes of azide and cyanamide are totally different. For cyanamides, the highest frequency ($\nu_{\text{sym.}} = 1301\,cm^{-1}$) is observed in $MgCN_2$ [37], while for azides the symmetric stretch modes are at higher frequency except in α-$Hg(N_3)_2$ ($\nu_{\text{sym.}} = 1275/1285\,cm^{-1}$) [39]. The Raman spectrum is shown in Fig. 4 and a comparison of Raman spectra of $Ba_3Na_2(CN_2)_4$ with other related cyanamides is listed in Table 5. In the title compound, the largest $\nu_{\text{sym.}}$ ($1241.5\,cm^{-1}$) and 2δ ($1356.4\,cm^{-1}$) correspond well with those of other cyanamide compounds. The $\nu_{\text{sym.}}$ and 2δ split into three and five peaks, respectively, because there are five crystallographically distinguishable cyanamide anions. As shown in Fig. 4 and Table 5, there is no doubt about the correctness of the cyanamide model. In general, since azides are thermally stable at atmospheric pressure only to 270–390 °C, it is not likely that azides could be prepared under our higher temperature (800 °C) reaction condition.

Although we could not obtain a pure single phase by varying reaction conditions, we successfully solved the single crystal structure of $Ba_3Na_2(CN_2)_4$ and confirmed the presence of cyanamide anions by Raman spectroscopy.

Acknowledgments

This work was supported by the National Science Foundation through Grant no. DMR-0245462. We thank Dr. E. Lobkovsky (single-crystal diffraction), N.I. Agladze (Raman Spectroscopy), and J. Hunt (SEM microprobe) for the use of their facilities at Cornell University. The SEM microprobe is one of the Cornell Center for Materials Research shared experimental facilities, supported through the National Science Foundation Materials Research Science and Engineering Center Program (DMR-0520404). Y.D. acknowledges support by the Kwanjeong Educational Foundation (studying abroad scholarship) in South Korea.

References

[1] P.E. Rauch, A. Simon, Angew. Chem. Int. Ed. 31 (1992) 1519–1521.
[2] G.J. Snyder, A. Simon, J. Am. Chem. Soc. 117 (1995) 1996–1999.
[3] G.J. Snyder, A. Simon, Angew. Chem. Int. Ed. 33 (1994) 689–691.
[4] J.M. Oliva, J. Solid State Chem. 178 (2005) 1023–1029.
[5] P. Höhn, R. Ramlau, H. Rosner, W. Schnelle, R. Kniep, Z. Anorg. Allg. Chem. 630 (2004) 1704.
[6] M. Kirchner, F.R. Wagner, W. Schnelle, R. Niewa, Z. Anorg. Allg. Chem. 630 (2004) 1735.
[7] H. Yamane, S. Sasaki, S. Kutoba, T. Kajiwara, M. Shimada, Acta Crystallogr. C 58 (2002) i50–i52.
[8] G. Cordier, M. Ludwig, D. Stahl, P.C. Schmidt, R. Kniep, Angew. Chem. Int. Ed. 34 (1995) 1761–1763.
[9] H. Yamane, S. Sasaki, T. Kajiwara, T. Yamada, M. Shimada, Acta Crytallogr. E 60 (2004) i120–i123.
[10] A. Schlechte, Yu. Prots, R. Niewa, Z. Kristallogr. New Cryst. Struct. 219 (2004) 349–350.
[11] M.S. Bailey, F.J. DiSalvo, J. Alloys Compd. 353 (2003) 146–152.
[12] G. Cordier, S. Rönninger, Z. Naturforsch. 42b (1987) 825–827.
[13] G. Cordier, Z. Naturforsch. 43b (1988) 1253–1255.
[14] H. Yamane, S. Sasaki, S. Kutoba, R. Inoue, M. Shimada, T. Kajiwara, J. Solid State Chem. 163 (2002) 449–454.
[15] H. Yamane, S. Sasaki, S. Kutoba, M. Shimada, T. Kajiwara, J. Solid State Chem. 170 (2003) 265–272.
[16] M.S. Bailey, D.Y. Shen, M.A. McGuire, D.C. Fredrickson, B.H. Toby, F.J. DiSalvo, H. Yamane, S. Sasaki, M. Shimada, Inorg. Chem. 44 (2005) 6680–6690.

[17] N.S.P. Watney, Z.A. Gál, M.D.S. Webster, S.J. Clarke, Chem. Commun. 33 (2005) 4190–4192.
[18] O. Reckeweg, F.J. DiSalvo, Angew. Chem. Int. Ed. 39 (2000) 412–414.
[19] O. Reckeweg, F.J. DiSalvo, Z. Naturforsch. 58b (2003) 201–204.
[20] Z.A. Gál, P.M. Mallinson, S.J. Clarke, Acta Crytallogr. E 61 (2005) i221–i222.
[21] O. Reckeweg, A. Simon, Z. Naturforsch. 58b (2003) 1097–1104.
[22] F. Zuercher, R. Nesper, S. Hoffmann, T. Faessler, Angew. Chem. Int. Ed. 34 (1995) 2703–2705.
[23] Bruker, APEX2 (version 1.22): Software for the CCD system, Bruker Analytical X-ray System, Madison, WI, 2004.
[24] Bruker, SAINT Plus: Software for the CCD system, Bruker Analytical X-ray System, Madison, WI, 2003.
[25] G.M. Sheldrick, SADABS, Institute für Anorganische Chemie der Universität Göttingen, Göttingen, Germany, 2003.
[26] Bruker, XPREP (version 6.14): Bruker Analytical X-ray System, Madison, WI, 2003.
[27] Y. Le Page, J. Appl. Crystallogr. 20 (1987) 264–269;
Y. Le Page, J. Appl. Crystallogr. 21 (1988) 983–984.
[28] A.L. Spek, PLATON. A Multipurpose Crystallographic Tool, Utrecht University, Utrecht, The Netherlands, 1999.
[29] G.M. Sheldrick, SHELXS97 and SHELXL97, University of Göttingen, Germany, 1997.
[30] L.J. Farrugia, J. Appl. Crystallogr. 32 (1999) 837–838.
[31] L.M. Gelato, E. Parthé, J. Appl. Crystallogr. 20 (1987) 139–143.
[32] G.M. Ehrlich, Ph.D. Thesis, Cornell University, Ithaca, NY, 1995.
[33] V. Vohn, W. Kockelmann, U. Ruschewitz, J. Alloys Compd. 284 (1999) 132–137.
[34] M. Becker, J. Nuss, M. Jansen, Z. Anorg. Allg. Chem. 626 (2000) 2505–2508.
[35] R.D. Shannon, Acta Crytallogr. A 32 (1976) 751–767.
[36] D. Fischer, M. Jansen, Angew. Chem. Int. Ed. 41 (2002) 1755–1756.
[37] U. Berger, W. Schnick, J. Alloys Compd. 206 (1994) 179–184.
[38] U. Berger, W. Schnick, Z. Naturforsch. 51b (1996) 1–8.
[39] U. Müller, Z. Anorg. Allg. Chem. 399 (1973) 183–192.